Molecular Genetics & Genomic Medicine

Open Access

ORIGINAL ARTICLE

Candidate gene analysis using genomic quantitative PCR: identification of *ADAMTS13* large deletions in two patients with Upshaw-Schulman syndrome

Yuka Eura[1], Koichi Kokame[1], Toshiro Takafuta[2], Ryojiro Tanaka[3], Hikaru Kobayashi[4], Fumihiro Ishida[5], Shuichi Hisanaga[6], Masanori Matsumoto[7], Yoshihiro Fujimura[7] & Toshiyuki Miyata[1]

[1]Department of Molecular Pathogenesis, National Cerebral and Cardiovascular Center, Suita, Osaka, Japan
[2]Department of Hematology and Clinical Immunology, Nishi-Kobe Medical Center, Kobe, Hyogo, Japan
[3]Department of Nephrology, Hyogo Prefectural Kobe Children's Hospital, Kobe, Hyogo, Japan
[4]Department of Hematology, Nagano Red Cross Hospital, Nagano, Japan
[5]Department of Biomedical Laboratory Sciences, Shinshu University School of Medicine, Matsumoto, Nagano, Japan
[6]Department of Nephrology, Koga General Hospital, Miyazaki, Japan
[7]Department of Blood Transfusion Medicine, Nara Medical University, Kashihara, Nara, Japan

Keywords
ADAMTS13, genetic analysis, hereditary disease, mutation, quantitative PCR, thrombotic thrombocytopenic purpura, Upshaw-Schulman syndrome

Correspondence
Koichi Kokame, Department of Molecular Pathogenesis, National Cerebral and Cardiovascular Center, Suita, Osaka 565-8565, Japan.
Tel: +81 6 6833 5012; Fax: +81 6 6835 1176; E-mail: kame@ncvc.go.jp

Funding Information
Y. E. was a research resident supported by the Association for Preventive Medicine of Japan at the National Cerebral and Cardiovascular Center. This work was supported in part by grants from the Ministry of Health, Labour, and Welfare of Japan; from the Ministry of Education, Culture, Sports, Science, and Technology of Japan; from Japan Society for the Promotion of Science; and from the Takeda Science Foundation.

Received: 1 November 2013; Revised: 18 December 2013; Accepted: 19 December 2013

Molecular Genetics & Genomic Medicine
2014; 2(3): 240–244

doi: 10.1002/mgg3.64

Abstract

Direct sequencing is a popular method to discover mutations in candidate genes responsible for hereditary diseases. A certain type of mutation, however, can be missed by the method. Here, we report a comprehensive genomic quantitative polymerase chain reaction (qPCR) to complement the weakness of direct sequencing. Upshaw-Schulman syndrome (USS) is a recessively inherited disease associated with severe deficiency of plasma ADAMTS13 activity. We previously analyzed *ADAMTS13* in 47 USS patients using direct sequencing, and 44 of them had either homozygous or compound heterozygous mutations. Then, we sought to reveal more extensive defects of *ADAMTS13* in the remaining three patients. We quantified copy numbers of each *ADAMTS13* exon in the patients by using genomic qPCR. Each primer pair was designed to contain at least one of the two primers used in direct sequencing, to avoid missing any exonic deletions. The qPCR demonstrated heterozygous loss of exons 7 and 8 in one patient and exon 27 in the other, and further analysis revealed c.746_987+373del1782 and c.3751_3892+587del729, respectively. Genomic qPCR provides an effective method for identifying extensive defects of the target genes.

Target exon resequencing using direct sequencing is a popular method to discover causative mutations in the candidate genes responsible for hereditary diseases. Homozygous or compound heterozygous mutations are often identified in the corresponding genes of the patients with autosomal-recessive diseases. In some cases, however, only one or no causative mutation is identified in the responsible gene: (an)other mutation(s) may be

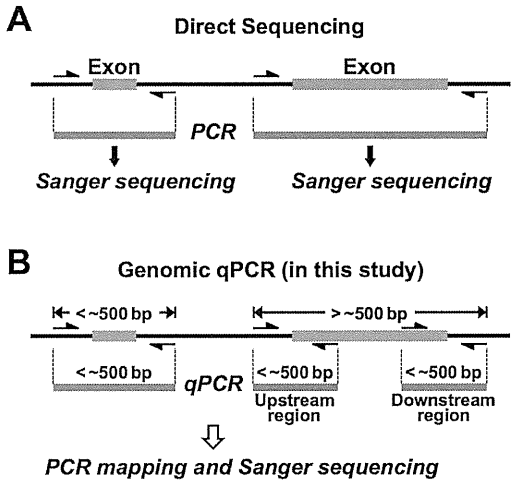

Figure 1. Principles of direct sequencing and genomic qPCR for genetic analysis. (A) In direct sequencing, target regions are amplified by PCR using primer pairs (arrows) usually designed from the intronic sequences flanking each exon, and the PCR products are directly sequenced by the Sanger method. (B) In genomic qPCR, copy numbers of target regions are quantified by real-time PCR. Each primer pair contains at least one of the two primers used in direct sequencing: common primer pairs are used for the regions smaller than ~500 bp, and, for accurate qPCR, one common and one specific primer are used for the regions larger than ~500 bp. If abnormal copy numbers are detected, PCR mapping and sequencing are performed to determine the precise sites of defects.

missed by the method. Although next-generation sequencing may be useful in such cases, it needs special equipments and is still expensive. In this study, we report a comprehensive genomic quantitative PCR (qPCR), which will be a powerful tool in combination with direct sequencing.

Upshaw-Schulman syndrome (USS), also called hereditary thrombotic thrombocytopenic purpura (TTP), is an autosomal-recessive trait associated with severely deficient plasma ADAMTS13 activity. Homozygous or compound heterozygous mutations in the *ADAMTS13* gene (OMIM 604134) are identified in most patients with USS (Levy et al. 2001; Kokame et al. 2002; Kokame and Miyata 2004; Matsumoto et al. 2004; Lotta et al. 2010; Fujimura et al. 2011; Hing et al. 2013). So far, more than 130 causative mutations have been identified by direct sequencing. Using that method, we previously analyzed *ADAMTS13* in 47 Japanese USS patients from 41 unrelated families (Fujimura et al. 2011). Of those, 44 patients from 38 families had either homozygous or compound heterozygous mutations in *ADAMTS13*. In the remaining three patients, however, only single missense mutations (two patients) or no mutation (one patient) was detected. In this study, we sought to reveal more extensive defects of *ADAMTS13* in these three patients by using genomic qPCR.

In general, PCR primer pairs for direct sequencing are designed to hybridize within the intronic sequences flanking each exon (Fig. 1A). Mutations such as substitutions, insertions, and deletions occurring in exons and exon–intron boundaries are identified by Sanger sequencing following genomic PCR, regardless of their heterozygosity or homozygosity (Fig. S1A). Direct sequencing, however, misses heterozygous mutations on the allele that contains no or mismatched primer target sequences: not only whole or partial deletion but also point mutations including single-nucleotide polymorphisms of primer target sequences can hamper PCR-amplification of the mutant allele, which may contain other critical mutations in the exon or exon–intron boundary (Fig. S1B). In these cases, only the target region of the other (normal) allele is PCR-amplified and sequenced, and the results are interpreted as if the regions of both alleles are normal.

Copy number analysis may overcome the limitations of direct sequencing. Multiplex ligation-dependent probe amplification (MLPA) analysis (Schouten et al. 2002) is often used for this purpose. Although MLPA is suitable for detection of genetic defects including exon deletions and duplications, it may still miss mutations that occur outside the probe target sequences. Therefore, to comple-

Figure 2. Genetic analysis of three USS families. (A) Pedigrees and genotypes of the USS patient families. Circles with arrows indicate the probands, USS-W4, -X5, and -KK3. Clinical data of the patients and the basis of diagnosis were described previously (Fujimura et al. 2011); the description of USS-KK3 being the second of three children needs to be corrected. Plasma ADAMTS13 activities were measured by us (USS-W and -X) or by Dr. Miha Furlan at University of Bern in 1999 (USS-KK), and are shown as a percentage of the normal control. ND, not determined. No subjects had ADAMTS13 inhibitors. Squares and circles with numbers indicate the subjects for genetic analysis. Each mutation was assigned a name for cDNA according to the nomenclature recommendations of the HGVS (http://www.hgvs.org/mutnomen/) based on the reference sequences AB069698.2 (cDNA) and NC_000009.11 (genomic). *,§Missense substitutions identified by direct sequencing. †Deletions identified by genomic qPCR in this study. *Pathologically unrelated missense polymorphisms. (B) Identification of exon deletions in *ADAMTS13*. Ct values of genomic qPCR are plotted by dots with lines at the mean (n = 2) for each target region. The letters u and d following the exon numbers indicate *u*pstream and *d*ownstream region of each exon, respectively. Red circles, USS-W4; green squares, USS-X5; blue triangles, USS-KK3. Arrows indicate the dots with Ct values higher than those of the other two patients. (C) *Left*: PCR-amplification of the 3.6-kbp band from the normal *ADAMTS13* allele produced a 1.8-kbp band from USS-W4, her mother (W2) and her brother (W3), but not from her father (W1). *Right*: PCR-amplification of the 1.2-kbp band from the normal *ADAMTS13* allele produced a 0.5-kbp band from USS-KK3, but not from her mother (KK2). (D) Sequencing of the 1.8- and 0.5-kbp bands in (C) indicated a 1782-bp deletion in USS-W4 and a 729-bp deletion in USS-KK3, respectively.

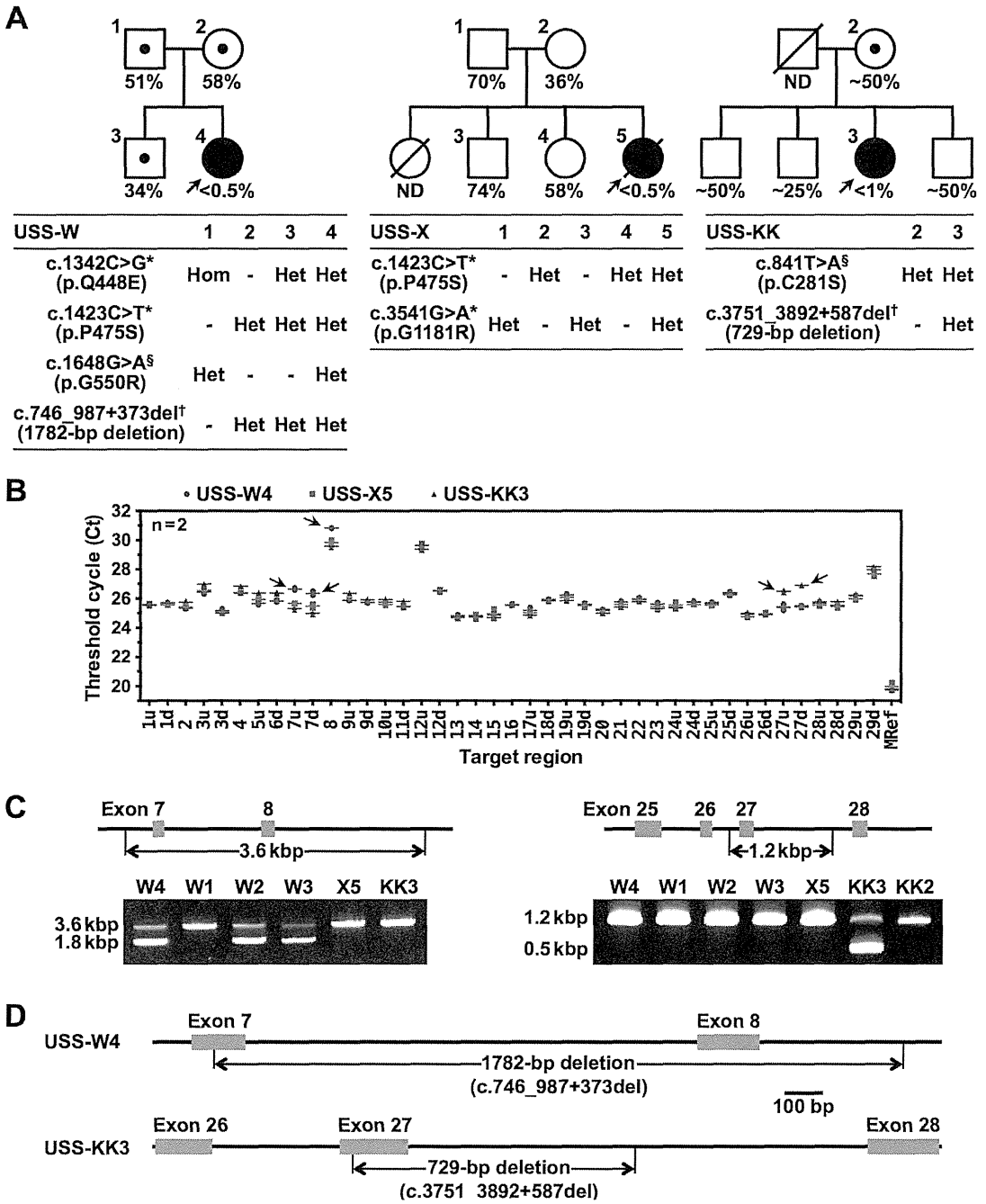

ment direct sequencing, we selected genomic qPCR (Aldape et al. 2002; Kuramitsu et al. 2012), using primer pairs containing at least one of the two primers used in direct sequencing (Fig. 1B). Combining direct sequencing and genomic qPCR should reveal any defects occurring within or between primer target sequences.

The study protocol was approved by the ethical committee of the National Cerebral and Cardiovascular Center; only subjects who provided written informed consent for genetic analyses were included. This study involved three USS families, USS-W, -X, and -KK (Fig. 2A). Clinical data of the patients (USS-W4, -X5, and -KK3) and the basis of diagnosis were described previously (Fujimura et al. 2011). Plasma ADAMTS13 activities for patients and family members are shown in Figure 2A. No subjects had ADAMTS13 inhibitors. The results of direct sequenc-

ing are also shown in Figure 2A. USS-W4 was a heterozygote with paternal c.1648G>A (p.G550R), USS-X5 had no causative mutations, and USS-KK3 was a heterozygote with maternal c.841T>A (p.C281S). Pathologically unrelated missense polymorphisms (p.Q448E, p.P475S, p.G1181R) (Kokame et al. 2011) were also identified in them (Fig. 2A).

Genomic DNA was prepared from blood and subjected to real-time PCR to quantify the copy numbers of each *ADAMTS13* exon. Each primer pair was designed, using Primer-BLAST (NCBI), to contain at least one of two primers used in direct sequencing (Table S1). A primer pair for the qBiomarker Multicopy Reference Copy Number Assay (MRef, Qiagen, Valencia, CA), which recognizes a stable sequence that appears >60 times throughout the human genome, was used to precisely normalize sample DNA input (~4 ng/reaction). PCR was performed using the QuantiFast SYBR Green PCR Kit (Qiagen) for all regions except exon 7 and the KOD SYBR qPCR Mix (Toyobo, Osaka, Japan) for exon 7. Dimethyl sulfoxide was added (final concentration, 5%) for amplification of exon 8. Fluorescence intensities were detected using the Mx3000P QPCR System (Agilent Technologies, Santa Clara, CA), and each threshold cycle (Ct) value was calculated using the MxPro software (Agilent Technologies).

In genomic qPCR, the difference in Ct among subject DNAs is important information. An increase in Ct value of 1.0 indicates a heterozygous deletion of the target region, whereas a decrease of 0.58 indicates a heterozygous duplication. Ct values of the *ADAMTS13* qPCR indicated that exons 7 and 8 were heterozygously absent in USS-W4 and that exon 27 was heterozygously absent in USS-KK3 (Fig. 2B). By contrast, genomic qPCR revealed no abnormalities in USS-X5.

To confirm the deletions and narrow the deleted regions, we performed PCR using primer pairs specific to regions surrounding the deleted exons. Primers 5′-CACCTCCCCACAGACTCCTA-3′ (intron 6) and 5′-AGGCGGGCAAATCATGAGG-3′ (intron 8) amplified a 3.6-kbp band from the normal allele and a 1.8-kbp band from the mutant allele of USS-W4 (Fig. 2C, *left*). Thus, ~1.8 kbp was deleted within the region straddling exons 7 and 8 in USS-W4. The precise sites where the deletions occurred were determined by sequencing the lower PCR band, which revealed that loss of exons 7 and 8 was caused by a 1782-bp deletion ranging from the 60th nucleotide of exon 7 to the 373rd nucleotide of intron 8 (c.746_987+373del1782) (Figs. 2D, S2A). We confirmed the compound heterozygosity of p.G550R and c.746_987+373del1782 in USS-W4 by genomic PCR of the family members. The patient's mother and brother, but not father, had c.746_987+373del1782 (Fig. 2C, *left*). Direct sequencing indicated that the patient's father, but not mother and brother, had p.G550R (Fig. 2A, *left*).

On the other hand, primers 5′-AGTCACATAGCCAGCAGTGG-3′ (intron 26) and 5′-GCACTGAGCAGAGTGGTCTT-3′ (intron 27) amplified a 1.2-kbp band from the normal allele and a 0.5-kbp band from the mutant allele of USS-KK3 (Fig. 2C, *right*). Thus, ~0.7 kbp was deleted within the region straddling exon 27 in USS-KK3. Sequencing the lower band revealed that loss of exon 27 was caused by a 729-bp deletion ranging from the 36th nucleotide of exon 27 to the 587th nucleotide of intron 27 (c.3751_3892+587del729) (Figs. 2D, S2B). Although the patient's father could not be genetically analyzed, her mother had p.C281S (Fig. 2A, *right*), but not c.3751_3892+587del729 (Fig. 2C, *right*). Thus, it was likely that USS-KK3 was a compound heterozygote of p.C281S and c.3751_3892+587del729.

In conclusion, this study identified two USS patients carrying *ADAMTS13* alleles bearing exon deletions. Extensive defects of *ADAMTS13* may be more common than we expect, and genomic qPCR analysis will be effective for identifying such defects in USS patients. Of the three patients we examined, one did not exhibit abnormalities detectable by either direct sequencing or genomic qPCR. Because these combined analytical methods cannot detect large-scale events such as inversions and translocations that do not affect sequences or copy numbers of target regions, the patient may carry such a defect in *ADAMTS13*. Alternatively, plasma ADAMTS13 deficiency in the patient may be brought about by defects other than *ADAMTS13*, for example, genes involved in synthesis, folding, or secretion of ADAMTS13. Finally, we propose well-designed comprehensive genomic qPCR to complement the weakness of direct sequencing of candidate genes.

Acknowledgments

We thank Ayami Isonishi for her technical assistance. Y. E. was a research resident supported by the Association for Preventive Medicine of Japan at the National Cerebral and Cardiovascular Center. This work was supported in part by grants from the Ministry of Health, Labour, and Welfare of Japan; from the Ministry of Education, Culture, Sports, Science, and Technology of Japan; and from Japan Society for the Promotion of Science.

Conflict of Interest

M. M. is a clinical advisory board for Alexion Pharmaceuticals. Y. F. is a clinical advisory board for Baxter Bioscience and for Alexion Pharmaceuticals.

References

Aldape, K., D. G. Ginzinger, and T. E. Godfrey. 2002. Real-time quantitative polymerase chain reaction: a potential tool for genetic analysis in neuropathology. Brain Pathol. 12:54–66.

Fujimura, Y., M. Matsumoto, A. Isonishi, H. Yagi, K. Kokame, K. Soejima, et al. 2011. Natural history of Upshaw-
Schulman syndrome based on *ADAMTS13* gene analysis in Japan. J. Thromb. Haemost. 9(Suppl. 1):283–301.

Hing, Z. A., T. Schiller, A. Wu, N. Hamasaki-Katagiri, E. B. Struble, E. Russek-Cohen, et al. 2013. Multiple in silico tools predict phenotypic manifestations in congenital thrombotic thrombocytopenic purpura. Br. J. Haematol. 160:825–837.

Kokame, K., and T. Miyata. 2004. Genetic defects leading to hereditary thrombotic thrombocytopenic purpura. Semin. Hematol. 41:34–40.

Kokame, K., M. Matsumoto, K. Soejima, H. Yagi, H. Ishizashi, M. Funato, et al. 2002. Mutations and common polymorphisms in *ADAMTS13* gene responsible for von Willebrand factor-cleaving protease activity. Proc. Natl. Acad. Sci. USA 99:11902–11907.

Kokame, K., Y. Kokubo, and T. Miyata. 2011. Polymorphisms and mutations of *ADAMTS13* in the Japanese population and estimation of the number of patients with Upshaw-Schulman syndrome. J. Thromb. Haemost. 9:1654–1656.

Kuramitsu, M., A. Sato-Otsubo, T. Morio, M. Takagi, T. Toki, K. Terui, et al. 2012. Extensive gene deletions in Japanese patients with Diamond-Blackfan anemia. Blood 119:2376–2384.

Levy, G. G., W. C. Nichols, E. C. Lian, T. Foroud, J. N. McClintick, B. M. McGee, et al. 2001. Mutations in a member of the *ADAMTS* gene family cause thrombotic thrombocytopenic purpura. Nature 413:488–494.

Lotta, L. A., I. Garagiola, R. Palla, A. Cairo, and F. Peyvandi. 2010. *ADAMTS13* mutations and polymorphisms in congenital thrombotic thrombocytopenic purpura. Hum. Mutat. 31:11–19.

Matsumoto, M., K. Kokame, K. Soejima, M. Miura, S. Hayashi, Y. Fujii, et al. 2004. Molecular characterization of *ADAMTS13* gene mutations in Japanese patients with Upshaw-Schulman syndrome. Blood 103:1305–1310.

Schouten, J. P., C. J. McElgunn, R. Waaijer, D. Zwijnenburg, F. Diepvens, and G. Pals. 2002. Relative quantification of 40 nucleic acid sequences by multiplex ligation-dependent probe amplification. Nucleic Acids Res. 30:e57.

Supporting Information

Additional Supporting Information may be found in the online version of this article:

Table S1. Primer pairs for *ADAMTS13* genomic qPCR.

Figure S1. Combinatorial analysis of direct sequencing and genomic qPCR should catch any defects occurring on and between the primer target sequences. Direct sequencing detects mutations such as point mutations (including substitutions, insertions, and deletions), short insertions, and deletions in the exons and exon–intron boundaries (A), but misses mutations on the allele that contains no or mismatched primer target sequences (B). Genomic qPCR for quantifying the copy numbers of target regions complements the results of direct sequencing.

Figure S2. Deleted regions and flanking sequences of *ADAMTS13* identified in two patients with USS. The 1782- and 729-bp regions (red letters) were deleted in patients USS-W4 (A) and USS-KK3 (B), respectively. Lowercase and uppercase sequences indicate introns and exons, respectively. Underlined sequences adjacent to the breakpoints may cause microhomology-mediated end joining (MMEJ) (McVey and Lee. Trends Genet. 2008;24:529–538).

Table S1 Primer pairs for *ADAMTS13* genomic qPCR

Exon number	Forward primer	Reverse primer	Product size (bp)
1u	gattgccaggccgtttgtgat*	CAGTATGGAATGGGACAGGC	356
1d	CATCTTAGAGCAAGGCCCAG	gcaaaccccaaagctgatgta*	432
2	cctcggtctccccaagtgtta*	gaaccctggcctggctggaac*	348
3u	ggtgggggtgacacgcaatgt*	gagagcaagcagtggaaagc	92
3d	catccttccaagacctgcca	ccaggggagggagggagaaga*	400
4	tgttttccttgcgttagttgg*	gaggatggagatgcgatgact*	382
5u	aacaaaccgaccgcagtcagc*	catcagaaagctcggctacC	216
6d	tctctcaccgagGTTTGACC	ggttcccctgtcctcacacct*	317
7u	gctggcgctgcggcactaggg*	TCCGAAGCCATCACGTGTC	184
7d	TGAGCCTGCTCAGgtagc	gttggacggaggggtgggttg*	159
8	actcctccgtcccgcctcctc*	gccctcccaggactagctaca*	477
9u	gtgcagagtgttggctgtgtc*	AGGGCCTGGCACATATCcta	137
9d	TGGATGGGACAGAATGTGGC	ctctgccccatactggtcctg*	138
10u	tgaggatgttgggggactctc*	gtacCTGGGGTTGTTGCACT	245
11d	tccctagttgaaggcagtgg	caaatgtgtcctggtgtgaac*	222
12u	tgaggccacacccacatcttg*	cctatgactctgccctgtcc	312
12d	tcggacagggcagagtcata	atgccagagcctgaaccactt*	76
13	atagaaaccccttgccccagat*	atccttttccccagcaccact*	390
14	cagggctgcagagtcattgag*	gaagggtggcgaagtggaaga*	358
15	ctcccctttgtctgtggtgtgg*	actatcaagcctgagggtggt*	279
16	gggaccccgggaaggagagtc*	gtaagtgaccgctgaatgaat*	393
17u	gcttgctgaacgaaagattat*	CGTGGCTTAGGCTGGAAGT	201
18d	CAGGAAGGAGTTGGTGGAGA	cagtgtcctcacctgcagaat*	288
19u	accagcctgtgattcggttgt*	GGGGCAATGTCTTCAGGAG	298
19d	acgctctgtctccttcctca	aggaactctgacagcagcact*	381
20	ctctttgggctcctggatgtt*	caatgggtgctcctcgttctc*	386
21	aaggatacccgctgcgagacc*	agccaatcaacacccacattt*	489
22	ccatgcgggccttatgtgcta*	tctgggttgcagtcctcaaag*	439
23	gggggcctccagaaagagaac*	gtgttgcccaggttggacttg*	476
24u	ggctcagtggctgcactttcc*	AATGAGACAGGGGACACTGG	310
24d	agcctctctctggggtcttc	tccagcgtccccaaacctaag*	460
25u	gacagggacccagacttgaat*	CTGTGGTCCGTCCTGGAG	423
25d	tgggcaaaggcatcttcctc	aagttacttccccttgatagt*	146
26u	ctgcatgtgccccctcttgct*	CGCACTGCAGTTGAGAGAAC	374
26d	AGCCAACAGGAACCATTGAC	tgggcacatcacttaatctct*	322
27u	gtgcattcccacctgtagttt*	gcctggccatacCTCTGTAG	423
27d	GAGGAAGATGTGCAGGAAGC	tccctggcacgtgcagactga*	315
28u	ccagagcccagaacatttagc*	gggaaagctgtccagaatca	434
28d	AGTCCAGCCACGAGTAATGC	gccactatttcactcttgtag*	327
29u	gtgtccttggggaagtgatgt*	CCTCAGGTTCCTTCCTTTCC	397
29d	ACTGGGAGTCAGAGAGCAGC	gattggattttcttcctggat*	514

"u" and "d" following the exon numbers indicate upstream and downstream region of each exon, respectively.
Lowercase and uppercase letters indicate sequences within introns and exons, respectively.
Primers with an asterisk were also used for direct sequencing.

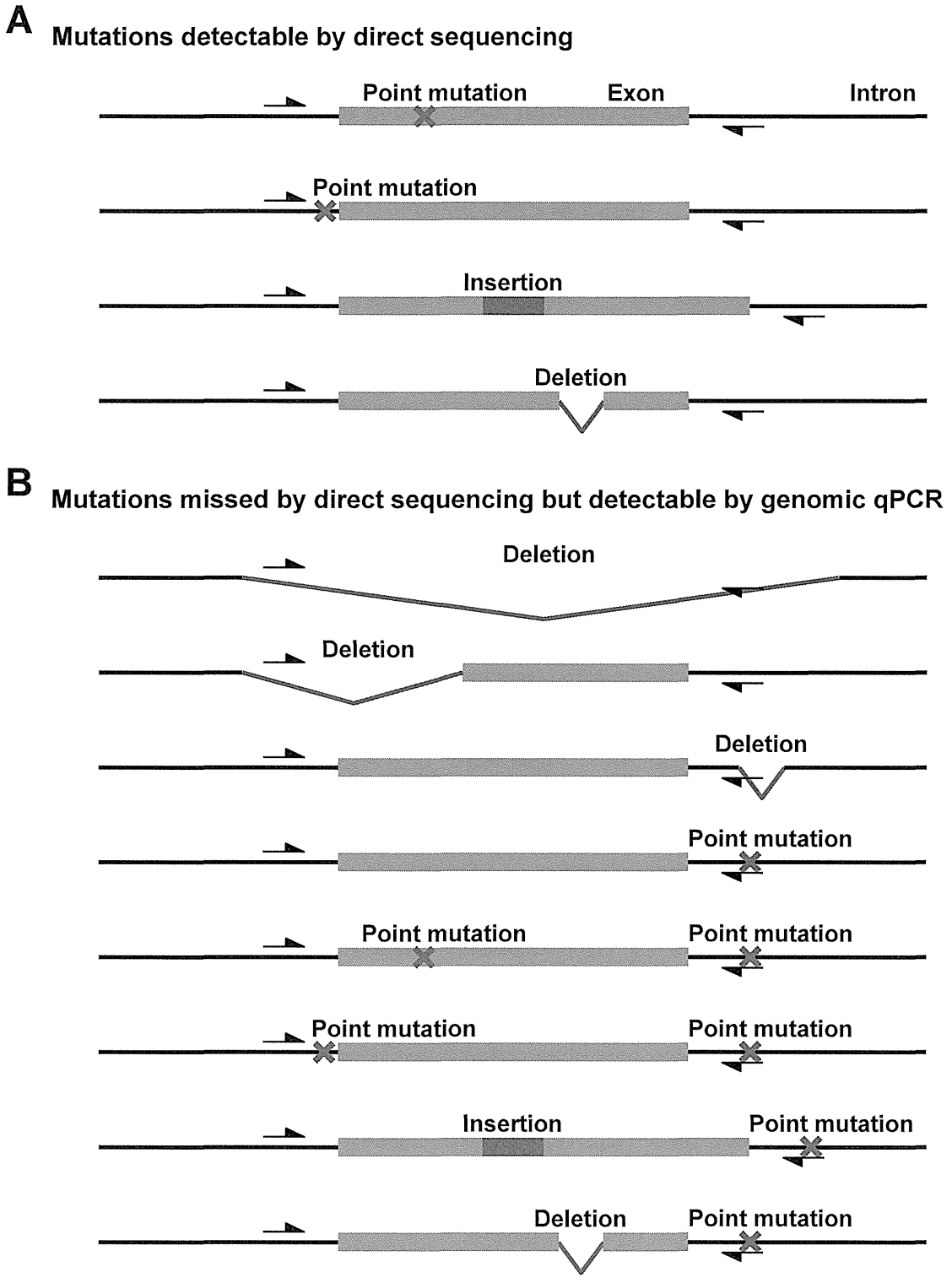

Figure S1. Combinatorial analysis of direct sequencing and genomic qPCR should catch any defects occurring on and between the primer target sequences. Direct sequencing detects mutations such as point mutations (including substitutions, insertions, and deletions), short insertions, and deletions in the exons and exon-intron boundaries (**A**), but misses mutations on the allele that contains no or mismatched primer target sequences (**B**). Genomic qPCR for quantifying the copy numbers of target regions complements the results of direct sequencing.

A **c.746_987+373del: 1782-bp deletion identified in the USS-W4 patient**

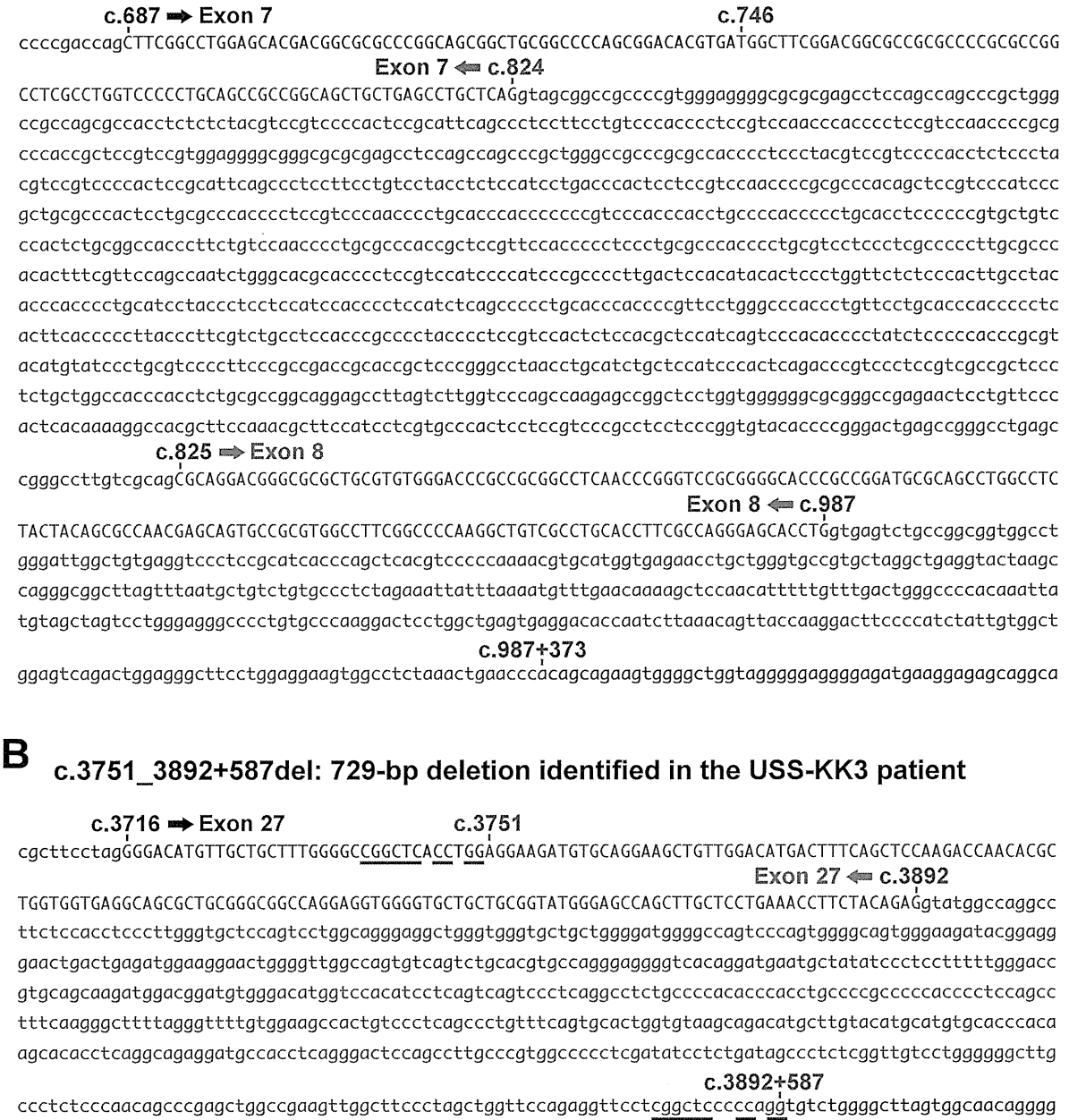

B **c.3751_3892+587del: 729-bp deletion identified in the USS-KK3 patient**

Figure S2. Deleted regions and flanking sequences of *ADAMTS13* identified in two patients with USS. The 1,782- and 729-bp regions (red letters) were deleted in patients USS-W4 (**A**) and USS-KK3 (**B**), respectively. Lowercase and uppercase sequences indicate introns and exons, respectively. Underlined sequences adjacent to the breakpoints may cause microhomology-mediated end joining (MMEJ) [McVey and Lee. Trends Genet. 2008; 24: 529–538].

Journal of Thrombosis and Haemostasis, **12**: 670–679 DOI: 10.1111/jth.12535

ORIGINAL ARTICLE

Identification of N-linked glycosylation and putative O-fucosylation, C-mannosylation sites in plasma derived ADAMTS13

N. SORVILLO,* P. H. KAIJEN,* M. MATSUMOTO,† Y. FUJIMURA,† C. VAN DER ZWAAN,* F. C. VERBIJ,* W. POS,*‡[1] R. FIJNHEER,§ J. VOORBERG*¶ and A. B. MEIJER***

**Department of Plasma Proteins, Sanquin-AMC Landsteiner Laboratory, Amsterdam, the Netherlands; †Department of Blood Transfusion Medicine, Nara Medical University, Kashihara City Nara, Japan; ‡Department of Cancer Immunology & AIDS, Dana-Farber Cancer Institute, Boston, MA, USA; §Department of Haematology, University Medical Center Utrecht, Utrecht; ¶Department of Vascular Medicine, University of Amsterdam, Amsterdam; and **Utrecht Institute for Pharmaceutical Sciences, Utrecht University, Utrecht, the Netherlands*

To cite this article: Sorvillo N, Kaijen PH, Matsumoto M, Fujimura Y, van der Zwaan C, Verbij FC, Pos W, Fijnheer R, Voorberg J, Meijer AB. Identification of N-linked glycosylation and putative O-fucosylation, C-mannosylation sites in plasma derived ADAMTS13. *J Thromb Haemost* 2014; **12**: 670–9

Summary. *Background:* Acquired deficiency of ADAMTS13 causes a rare and life-threatening disorder called thrombotic thrombocytopenic purpura (TTP). Several studies have shown that aberrant glycosylation can play an important role in the pathogenesis of autoimmune diseases. N-linked glycosylation and putative O-fucosylation sites have been predicted or identified in recombinant ADAMTS13. However, it is not known which of these sites are glycosylated in plasma derived ADAMTS13. *Objectives:* Here we investigated the presence of putative O-fucosylation, C-mannosylation and N-linked glycosylation sites on plasma derived ADAMTS13. *Methods/Results:* Sites of N-linked glycosylation were determined by the use of peptide N-glycosidase-F (PNGase F), which removes the entire carbohydrate from the side chain of asparagines. Nine of the 10 predicted N-linked glycosylation sites were identified in or near the metalloproteinase, spacer, thrombospondin type 1 repeat (TSR1) and the CUB domain of plasma ADAMTS13. Moreover, six putative O-fucosylated sites were identified in the TSR domains of plasma ADAMTS13 by performing searches of the tandem mass spectrometry (MS/MS) data for loss of hexose (162 Da), deoxyhexose (146 Da), or hexose-deoxyhexose (308 Da). The use of electron transfer dissociation (ETD) allowed for unambiguous identification of the modified sites. In addition to putative O-fucosylation and N-linked glycosylation, two putative C-mannosylation sites were identified within the TSR1 and TSR4 domains of ADAMTS13. *Conclusions:* Our data identify several glycosylation sites on plasma derived ADAMTS13. We anticipate that our findings may be relevant for the initiation of autoimmune reactivity against ADAMTS13 in patients with acquired TTP.

Keywords: ADAMTS-13 protein, human; autoimmune diseases; glycosylation; mass spectrometry; thrombotic thrombocytopenic purpura.

Correspondence: Jan Voorberg, Department of Plasma Proteins, Sanquin Research and Landsteiner Laboratory, Academic Medical Center, Plesmanlaan 125, 1066 CX Amsterdam, the Netherlands.
Tel.: +31 20 512 3122; fax: +31 20 512 3310.
E-mail: j.voorberg@sanquin.nl

[1]Current address: Department of Cancer Immunology & AIDS, Dana-Farber Cancer Institute, Boston, MA 02115, USA

Received 15 August 2013
Manuscript handled by: R. Camire
Final decision: P. H. Reitsma, 13 February 2014

Introduction

ADAMTS13 is a plasma metalloproteinase that regulates platelet adhesion and aggregation by its ability to process ultra-large von Willebrand factor (VWF) multimers on the surface of endothelial cells [1–3]. It is a member of the ADAMTS family (a disintegrinlike and metalloproteinase with thrombospondin type 1 repeats) and like most secreted proteins it is predicted to contain several N- and/or O-linked oligosaccharides [2]. Recent studies have shown that recombinant ADAMTS13 is highly glycosylated presenting both O-fucosylated and N-glycosylated residues. O-fucosylation (glucose-β (1,3)-fucose disaccharide linked to the hydroxyl group of Ser or Thr residues) occurs in at least 6 thrombospondin type 1 repeats (TSR) and is required for an appropriate secretion of the recombinant protease [4]. Several N-linked glycosylation sites (oligosaccharide chain linked through the N-acetylglucosamine group to an Asn residue) have been predicted throughout the entire protein:

two in the metalloproteinase domain (N142 and N146), four are in or near the spacer domain (N552, N579, N614 and N667), one in the second (N707) and fourth (N828) TSR, and two in the CUB domains (N1235 and N1354) [5]. N-linked glycans on recombinant ADAMTS13 play an important role in the secretion of ADAMTS13 but are not necessary for its VWF cleaving activity [5].

Deficiency of ADAMTS13 causes a rare and life-threatening disorder called thrombotic thrombocytopenic purpura (TTP). Patients affected by acquired TTP develop autoantibodies directed towards the metalloproteinase ADAMTS13 [6]. Reduced activity or absence of the metalloproteinase causes lack of cleavage of UL-VWF resulting in microvascular obstruction, low platelet counts (thrombocytopenia) and fragmentation of red blood cells (hemolytic anemia) [3,7,8]. Our current knowledge on the etiology of acquired TTP is limited. A large number of case reports suggest that microbial infections are linked to the onset or recurrence of this autoimmune disease [6].

Aberrant glycosylation of proteins can play an important role in the pathogenesis of autoimmune disorders [9]. Alterations in protein glycosylation may modify or create novel B-cell epitopes and may also influence the presentation of peptides to T-cells [10]. Previous work has shown that O-linked glycans can alter proteolytic processing and/or presentation of glycopeptides on MHC class II molecules and therefore interfere with activation of T-cells [11,12]. Glycosylated "self derived" peptides might not be presented efficiently by antigen presenting cells and might escape negative selection in the thymus [11]. However, in the periphery, modification of these peptides by glycosidases allows appropriate presentation of "self derived" peptides and activation of autoreactive T-cells leading to autoimmune reactivity towards self antigens [11].

Similarly, aberrant glycosylation of ADAMTS13 might contribute to the onset of acquired TTP by exposure of cryptic T-cell epitopes that are shielded by glycans under quiescent, non-inflammatory conditions. In this study we employed collision induced dissociation (CID) and electron transfer dissociation (ETD) to identify glycosylation sites in plasma derived ADAMTS13. Glycopeptide analysis by CID/ETD MS/MS identified nine N-linked sites in or near the metalloproteinase, spacer, thrombospondin type 1 repeat (TSR) and the CUB domain of plasma ADAMTS13. Six potential O-fucosylated sites were identified in the TSR domains of the protease. In addition to N-linked and potential O-fucosylated modifications, two putative C-mannosylation sites were identified within the TSR domains of ADAMTS13.

Materials and methods

Purification and deglycosylation of ADAMTS13

Full length recombinant ADAMTS13 was produced in stable HEK293 cells and purified as described previously [13]. Plasma ADAMTS13 was purified as described in the Supplemental Material and Method section using a specific monoclonal antibody A10 directed against the disintegrin domain of ADAMTS13 (Figure S1) [13,14]. Purified plasma and recombinant ADAMTS13 (200 nM) were incubated with PNGase F (2 U; Roche Diagnostics, Almere, the Netherlands) in a final volume of 50 μL, overnight at 37 °C in order to enzymatically remove N-linked sugar moieties from the protein. Removal of the glycans was assessed by SDS-PAGE on NuPAGE Bis-Tris Gel System 4–12% gel (Invitrogen, Breda, the Netherlands) followed by silver staining.

Generation of peptides and mass spectrometry sample preparation

Purified recombinant and plasma ADAMTS13 (200 nM) treated and non-treated with PNGase F (volume of 50 μL) was denatured by the addition of 6 M of urea (final concentration 2.4 M urea) for 15 min at room temperature. Urea concentration was reduced to 1 M by addition of 50 mM ammonium bicarbonate buffer (ABC). Disulfide bonds of the samples were reduced and alkylated by adding 10 μL of 100 mM 1.4-dithiothreitol freshly prepared in 50 mM ABC buffer for 30 min at room temperature following incubation with 25 μL of freshly prepared 55 mM iodoacetamide stock solution for 30 min at room temperature. Trypsin and chymotrypsin (Promega, Promega Benelux, the Netherlands) digestion was performed by incubation of the samples with 0.1 μg of the appropriate enzyme at room temperature. For chymotrypsin digestions 2.5 mM of $CaCl_2$ was added to the samples prior to addition of the enzyme. After overnight digestion the peptide mixtures were acidified with formic acid (Biosolve, Valkenswaard, the Netherlands) to stop the enzymatic reaction and to allow for concentration of the peptides using C18 zip tips (Millipore, Amsterdam, the Netherlands) as per the manufacturer's instructions. Peptides were eluted with acetonitrile that was subsequently removed from the samples before mass spectrometry analysis by evaporation under vacuum by speedvac centrifugation (Thermo Fisher Scientific, Bremen, Germany).

Mass spectrometry analysis of peptides

Peptides were separated using a reverse phase C18 column (50 μm × 20 cm, 5 μm particles; Nanoseparations, Nieuwkoop, the Netherlands) at a flow rate of 100 nl/min with a gradient from 0 to 35% (v/v) acetonitrile in 0.1 M hydrogen acetate. Eluted peptides were then sprayed directly into a LTQ XL Orbitrap mass spectrometer (Thermo Fisher Scientific Inc, Bremen, Germany) using a nanoelectrospray source with a spray voltage of 1.9 kV. Full mass spectrometry (MS) scans were performed and the five most intense precursor ions

from each full scan in the Orbitrap were selected for collision induced dissociation (CID; 300–2000 m/z, resolving power 30.000). Under CID fragmentation the peptide precursor ion undergoes one or more collisions by interactions with neutral gas molecules. The generated vibrational energy results in ion dissociation at the amide bonds along the peptide backbone generating b- and y-type fragment ions. Subsequently the product ions are ejected for detection, generating CID fragmentation spectra (MS/MS). Alternatively, the product ions can be kept and selected for another CID fragmentation, which can be repeated several times (MS^n were n indicates the number of CID reactions). MS/MS/MS was in fact triggered upon detection of neutral loss of the top 10 peptides in the MS/MS spectrum. For appropriate identification of the glycosylated sites several peptides were selected manually for electron transfer dissociation (ETD) fragmentation. This leads to the cleavage of N-Cα backbone bonds and generates c- and z- type fragment ions. In contrast to CID fragmentation, ETD fragmentation does not result in removal of intact oligosaccharide moieties from the peptide. The LTQ Orbitrap was calibrated on a monthly basis as recommended by the manufacturer in order to ensure a high mass accuracy.

Data analysis

Peptides were identified by screening each SEQUEST output file against the UniprotKB non-redundant protein 25.H_sapiens.fasta database using Proteome Discoverer version 1.2 software (Thermo Scientific, Bremen, Germany). Data were also analyzed against a decoy database from the 25.H_sapiens.fasta database comprising the reverse of all protein sequences. A false discovery rate (FDR) of 5% (which indicates that the probability that a peptide are false positive is <5%) was used as a cut-off for this study. The identification of oxidation on methionine (+15.994 Da; dynamic modification) and modification on cysteine groups (carbamidomethyl groups +57.0214 Da; static modification) was included during the search. Peptides modified by N-linked glycosylation were identified by the conversion of asparagine to aspartic acid at the site of carbohydrate attachment, resulting in an increase of the peptide mass of 1 Da (Asn → Asp; +0.9840). Identification of putative O-fucosylated sites was determined by performing searches for the hexose-deoxyhexose group (+308 Da) on serine residues. Tryptophans were monitored for the presence of a putative C-mannosylated group (+162.058). Individual MS/MS fragmentation spectra were manually analyzed in order to identify the sequential loss of hexose (162 Da), deoxyhexose (146 Da), or hexose-deoxyhexose (308 Da) from O-fucosylated sites and the loss of 120 Da in MS/MS spectra of peptides containing the modified tryptophan, a characteristic cross-ring fragmentation product of aromatic C-glycosides.

Results

Mapping of the N-linked glycosylation sites in plasma ADAMTS13

To identify N-linked glycosylation sites in plasma ADAMTS13 we used tandem MS to acquire mass/charge (m/z) values of peptides ions derived from in-solution tryptic and chymotryptic digestion of purified plasma ADAMTS13 after treatment with PNGase F. The enzyme is able to release the entire carbohydrate from the side chain of asparagine and in this process converts the amino acid asparagine to aspartic acid resulting in an increase of peptide mass of 1 Da. Treatment of purified plasma ADAMTS13 with PNGase F resulted in an increase of the sequence coverage from 72% towards 81% (Figure S2). Although PNGase F treatment increases ADAMTS13 sequence coverage not all peptides were detected. This is most probably due to the length of the peptides. Too long or extremely short peptides are out of range and not detectable by mass spectrometry. Full MS scans were performed and the five most intense precursor ions from each full scan were selected for CID and analyzed by MS/MS. Figure 1 illustrates the mass spectral data for the glycosylated peptide IAIHALATNMGAGTEGANASYILIR derived from the CUB2 domain of ADAMTS13. The series of b- and y-ions from the peptide confirm the presence of a glycan attached to N1354 for peptide I1337-R1361. Nine N-linked glycosylated peptides were identified throughout ADAMTS13 (Fig. 2). Mass spectra of the other N-linked peptides are provided in Figure S3. As shown in Fig. 2 two N-linked sites were identified in the metalloproteinase domain (N142 and N146), four in or near the spacer domain (N552, N579, N614 and N667), one in the second TSR domain (N707) and two in the CUB domains (N1235 and N1354). All peptides contained the N-glyco-

Fig. 1. Mapping of N-linked glycosylation sites in plasma ADAMTS13. Fragmentation spectra of deglycosylated peptide IAIHALATNMGAGTEGANASYILIR, derived from the CUB2 domain of ADAMTS13. Upper panel represents the MS/MS spectrum of the peptide. The peak corresponding to the parent ion is indicated in green; selected peaks corresponding to b- and y-ions are indicated in red and blue. The lower panel depicts the complete list of b- and y-ions. Theoretically predicted peptide masses are indicated in black. Y-ions that were found in the spectrum are indicated in blue whereas the b-ions that are indicated in red. Peptides masses highlighted in the spectrum are marked in yellow. Mass differences between Y_8^+ (950.53059) and Y_7^+ (835.50364) allows the identification of an Asp (monoisotopic mass: 115.02695) at position N1354 that is obtained after cleavage of N-linked glycans by PNGase F. Cleavage is obtained only when an Asn is modified by the addition of N-linked sugars. Cleavage by PNGase F converts an Asn to Asp resulting in an increase of peptide mass of 1 Da (from 114.04293 to 115.02695).

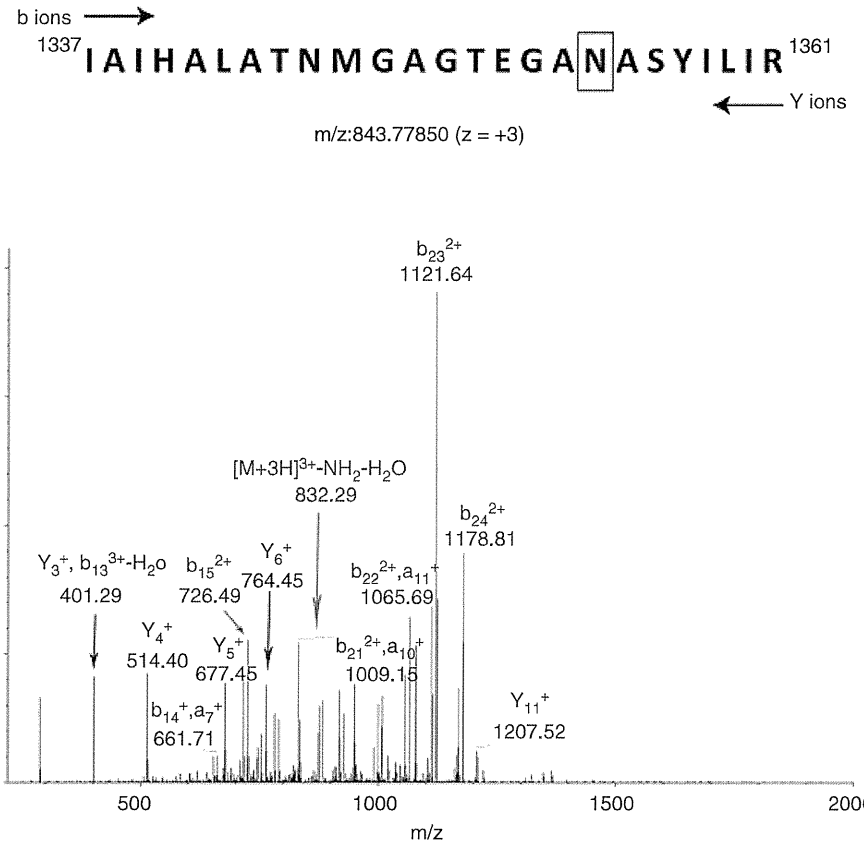

#1	b+	b2+	b3+	Seq.	y+	y2+	y3+	#2
1	114.09135	57.54931	38.70197	I				25
2	185.12847	93.06787	62.38101	A	2416.22904	1208.61816	806.08120	24
3	298.21254	149.60991	100.07570	I	2345.19192	1173.09960	782.40216	23
4	435.27145	218.13936	145.76200	H	2232.10785	1116.55756	744.70747	22
5	506.30857	253.65792	169.44104	A	2095.04894	1048.02811	699.02116	21
6	619.39264	310.19996	207.13573	L	2024.01182	1012.50955	675.34212	20
7	690.42976	345.71852	230.81477	A	1910.92775	955.96751	637.64743	19
8	791.47744	396.24236	264.49733	T	1839.89063	920.44895	613.96839	18
9	905.52037	453.26382	302.51164	N	1738.84295	869.92511	580.28583	17
10	1036.56087	518.78407	346.19181	M	1624.80002	812.90365	542.27152	16
11	1093.58234	547.29481	365.19896	G	1493.75952	747.38340	498.59136	15
12	1164.61946	582.81337	388.87800	A	1436.73805	718.87266	479.58420	14
13	1221.64093	611.32410	407.88516	G	1365.70093	683.35410	455.90516	13
14	1322.68861	661.84794	441.56772	T	1308.67946	654.84337	436.89800	12
15	1451.73121	726.36924	484.58192	E	1207.63178	604.31953	403.21544	11
16	1508.75268	754.87998	503.58908	G	1078.58918	539.79823	360.20124	10
17	1579.78980	790.39854	527.26812	A	1021.56771	511.28749	341.19409	9
18	1694.81674	847.91201	565.61043	N-Asn->Asp	950.53059	475.76893	317.51505	8
19	1765.85386	883.43057	589.28947	A	835.50364	418.25546	279.17273	7
20	1852.88589	926.94658	618.30015	S	764.46652	382.73690	255.49369	6
21	2015.94921	1008.47824	672.65459	Y	677.43449	339.22088	226.48301	5
22	2129.03328	1065.02028	710.34928	I	514.37117	257.68922	172.12857	4
23	2242.11735	1121.56231	748.04397	L	401.28710	201.14719	134.43388	3
24	2355.20142	1178.10435	785.73866	I	288.20303	144.60515	96.73919	2
25				R	175.11896	88.06312	59.04450	1

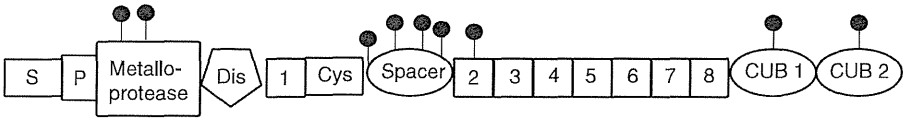

Glycosylation	Peptide sequence
N142+N146	MVILTEPEGAP**N**ITA**N**LTSSLVCGWSQTINPEDDTDPGHADLVLYSTR
N552	CQVCGGD**N**STCSPR
N579	AREYVTFLTVTP**N**LTSVYIANHRPLFTHLAVR
N614	MSISP**N**TTYPSLEEDGR
N667	YGEEYG**N**LTRPDITFTYFQPKPR
N707	WV**N**YSCLDQARK
N1235	VLESSL**N**CSAGDMLLLWGR
N1354	IAIHALATNMGAGTEGA**N**ASYILIR

Fig. 2. Schematic representation of the confirmed N-linked glycosylation sites in plasma derived ADAMTS13 measured by tandem MS.

sylation consensus sequence N-X-S/T and had an increase of mass of 1 Da. Interestingly, ADAMTS13 derived peptides containing the N-linked sites were identified only in samples treated with PNGase F with the exception of peptides containing N142, N146, N707 and N1354 that were also detected in non-PNGase F treated ADAMTS13. This observation suggests that N-glycosylation at these sites is not complete. We were not able to identify whether a glycan was attached to N828 since peptides containing this amino acid were not detected in our analysis. All nine N-linked glycosylation sites were also identified in recombinant ADAMTS13 that was analysed in parallel (Figure S4).

Detection of terminal sugars on both plasma and recombinant ADAMTS13 was carried out by assessing the binding of digoxygenin-labelled lectins. Lectins specifically recognizing terminal α-D-mannose (GNA), β-D-galactose (DSA) and terminal sialic acid (SNA and MAA) bound to both recombinant and plasma ADAMTS13 confirming the presence of complex and hybrid N-glycan structures on both proteins (Figure S5). The lectin PNA, that binds to the disaccharide galactose-β(1–3)-N-acetylgalactosamine, recognized recombinant but not plasma derived ADAMTS13. The disaccharide might not be accessible due to the presence of one or two sialic acids or by the addition of fucose, that needs to be removed enzymatically to allow binding of the PNA lectin. Absence of binding of this lectin suggests the presence of complex glycans structures on plasma ADAMTS13.

CID/ETD MS/MS analysis of putative O-fucosylation sites in plasma ADAMTS13

Chromatography and tandem mass spectrometry analysis have shown that the thrombospondin type 1 repeats (TSRs) of recombinant ADAMTS13 and from several other proteins are modified by the addition of the disaccharide glucose-β-(1–3)-fucose-α1-O linked to serine or threonine residues [4,15–18]. To determine whether the same modification occurs in plasma ADAMTS13 we examined tryptic and chymotryptic peptides derived from purified plasma ADAMTS13 through mass spectral analysis using two different fragmentation approaches: collision induced dissociation (CID) and electron transfer dissociation (ETD). CID fragmentation of the glycosylated peptides resulted in a characteristic pattern in accordance with the sequential neutral losses of hexose (Hex, 162 Da), deoxyhexose (dHex, 142 Da) and of the disaccharide hexose-deoxyhexose (Hex-dHex, 308 Da) (Fig. 3, Figure S6). As shown in Fig. 3, for TSR5-derived peptide TGAQAAHVWTPAAGSCSVSCGR (charge z = +2), the mass of the most intense ions in the spectrum (m/z 1116.72) corresponds to the loss of Hex-dHex disaccharide) with respect to the mass of the parent peptide ion (m/z 1270.06). The lower ions (m/z 1189 for TGAQAAHVWTPAAGSCSVSCGR) corresponds to the loss of the single Hex. MS/MS/MS fragmentation of the TGAQAAHVWTPAAGSCSVSCGR peptide without the Hex and dHex yields extensive peptide backbone fragments and provides sufficient information to appropriately identify the peptide (Fig. 3; right panel). Results from CID analysis suggested the presence of six putative O-fucosylated peptides within 6 of the 8 TSR domains of ADAMTS13 (Fig. 4 and Suppl. Figure S6). Formally, the observed neutral loss of Hex (162 Da) and dHex (142 Da) does not allow for identification of the attached glycan moiety. The identified glycosylation sites within the TSRs domain of ADAMTS13 fall within the consensus sequence of O-fucosylation depicted as WX5C1X2-3 (S/T)C2X2G. This suggests that the neutral losses correspond to the loss of fucose (162 Da), glucose (142 Da) and the disaccharide glucose-β(1–3)-fucose (Hex-dHex, 308 Da). Despite the fact that the TSR1 domain of ADAMTS13 contains a consensus sequence for O-fucosylation (CSRSCG) the peptide containing such modification was not retrieved in the mass spectrom-

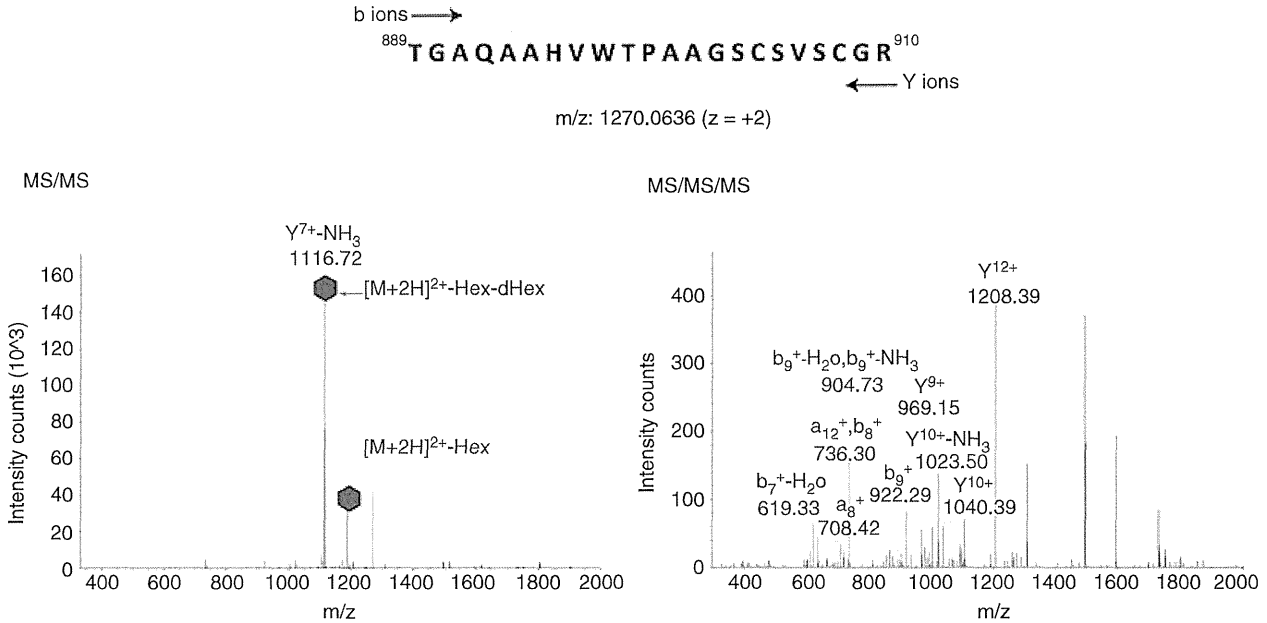

Fig. 3. Identification of putative O-fucosylation sites in TSR domains of ADAMTS13. Left panel represents the MS/MS spectrum of a tryptic peptide derived from the TSR5 domain of ADAMTS13. The major ions correspond to the sequential neutral loss of a hexose (81 Da; corresponding to loss of glucose from a doubly charged peptide; [M + 2H-Hex]2+, m/z 1.189) and of a hexose-deoxyhexose (154 Da loss of the glucose-fucose disaccharide from a double charged peptide; [M + 2H-Hex-dHex]2+, m/z 1116.72). Peaks corresponding to neutral losses are indicated by a red hexagon. Right panel shows the MS/MS/MS fragmentation confirming the assignment of the peptide. Selected peaks corresponding to b- and y-ions are indicated in red and blue.

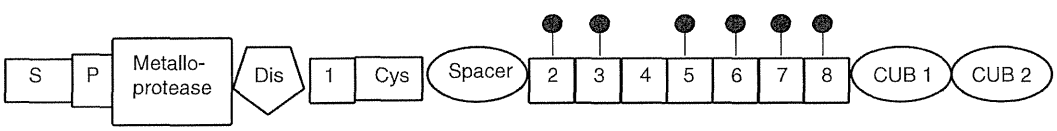

Glycosylation	Peptide sequence	Parent mass +H	Charge	Product mass +H	Parent - Observed
TSR 2	GPCSV**S**CGAGLR	1528.66	2	1220	308
TSR 3	ELVETVQCQGSQQPPAWPEACVLEPCPPYWAVGDFGPCSA**S**CGGGLR	5512.46	4	5207.48	305
TSR 5	TGAQAAHVWTPAAGSCSV**S**CGR	2539.12	2	2233.44	305.56
TSR 6	LAACSV**S**CGR	1288.6	2	1081.6	307
TSR 7	VMSLGPCSA**S**CGLGTAR	2047.29	2	1740.9	306.39
TSR 8	WHVGTWMECSV**S**CGDGIQR	2573.07	3	2267.28	305.79

Fig. 4. Schematic representation of potential O-linked fucosylation sites of plasma derived ADAMTS13.

etry analysis for both plasma and recombinant ADAMTS13. (Figure S6 and S7) [4]. No consensus site for putative O-fucosylation is present within TSR4. In accordance with the lack of a consensus site we did not obtain evidence for the presence of a potential O-fucosylation site in TSR4. MS/MS/MS spectra of Hex-dHex containing peptides derived from TSR2, TSR3 and TSR6 did not contain sufficient information to allow for appropriate identification of the modified amino acid (Figure S6; panel C, D and E). The same potential O-fucosylation sites were also identified for recombinant ADAMTS13 (Figure S7).

ETD fragmentation of glycosylated peptides produces several c- and z-ions (nomenclature of Zubarev and co-workers [19]), resulting from the cleavage of the N-Cα bonds, and allows the intact oligosaccharide moieties to remain attached to the fragment ions containing the glycans. The ETD process represents an excellent tool to allow the localization of sites of modification in glycopeptides. Therefore, the same putative O-linked fucosylated peptides identified by CID were analyzed by ETD. Figure 5 shows the ETD fragmentation of the Hex-dHex modified peptide GPCSVSCGAGLR derived from the TSR2 domain. Both c- and z- ions were observed

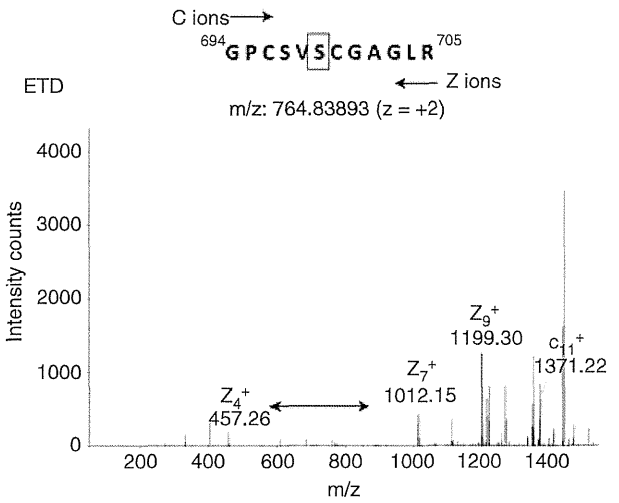

Fig. 5. Analysis of potential O-fucosylation of TSR domains of ADAMTS13 using ETD mass spectrometry. ETD spectrum of putative O-fucosylated peptide GPCSVSCGAGLR belonging to the TSR2 domain. The difference between z7+ and the z4+ is consistent with putative O-fucosylation of Ser698.

allowing sequence determination of the peptide. The glycosylation site was determined by the mass differences between z + 7 to z + 4 (indicated by the arrow). The ETD spectra obtained for peptides TGAQAAHVWTPAAGSCSVSCGR and WHVGTWMECSVSCGDGIR are depicted in Figure S8. Although the putative O-fucosylated modification sites were recognized as S698, S907 and S1087 respectively, ETD fragmentation of the glycosylated peptides of TSR5 and TSR8 suggested that these peptides can be modified at different sites: S691 and S695 for TGAQAAHVWTPAAGSCSVSCGR, S905 for WHVGTWMECSVSCGDGIR. This suggests the possibility of two positional isomers of the same peptide with putative O-fucosylation modifications on different residues. The ETD spectrum fragmentation for the remaining peptides derived from TSR3, TSR6 and TSR7 did not show extensive sequence coverage (data not shown) and therefore it was not possible to identify the exact site of modification. A consensus sequence for O-fucosylation has been defined previously as WX5C1X2-3(S/T)C2X2G [4,16]. Based on this consensus sequence the glycosylation sites for ELVETVQCQGSQQPAWPEACVLEPCPPYWAVGDFGPCSASCGGLR (TSR3), LAACSVSCGR (TSR6) and VMSLGPCSASCGLGTAR (TSR7) are most likely at S757, S965 and S1027, respectively.

C-mannosylation of plasma ADAMTS13

In addition to O-fucosylation TSRs often contain a consensus motif for C-mannosylation which has been defined as WXXW [15,16,18]. Examination of the sequence of ADAMTS13 suggests the presence of several potential C-mannosylation sites. We therefore analyzed ADAMTS13 derived peptides, obtained as described above, employing CID and ETD tandem mass spectrometry. Peptides carrying an additional 162 Da mass (suggested to correspond to a single mannosyl residue) were subjected to ETD fragmentation. Figure 6 and Figure S10 show the MS/MS fragmentation of respectively plasma and recombinant ADAMTS13 derived peptide: APSPWGSIR belonging to the TSR4 domain. Evidence for putative C-mannosylation of Trp884 was further suggested by the loss of 120 Da in the MS/MS spectra (Fig. 6; left panel), a characteristic cross-ring fragmentation product of aromatic C-glycosides. In addition, ETD-fragmentation was performed yielding a series of c- and z-ions that were consistent with the presence of C-mannose on Trp884 in the APSPWGSIR peptide (Fig. 6; right panel). Mass differences between z + 5 and z + 4 provided evidence for Trp884 as site of glycosylation. Evidence for a second putative C-mannosylation site at Trp390 in the WSSWGPR peptide in the TSR 1 domain was obtained (Figure S9 and S10) for both plasma and recombinant ADAMTS13.

Discussion

Like most secreted proteins ADAMTS13 undergoes post-translational modifications and is predicted to contain several N-linked oligosaccharides. In our current study we were able to demonstrate by means of tandem mass spectrometry that plasma ADAMTS13 is a highly glycosylated protein presenting several N-, O- and C-linked glycosylation sites. Treatment of plasma ADAMTS13 with PNGase F, which removes the N-linked glycan moieties, allowed for the identification of 9 out of 10 predicted N-linked glycosylation sites; two in the metalloproteinase domain (N142 and N146), four in or near the spacer domain (N552, N579, N614 and N667), one in the second TSR domain (N707) and two in the CUB domains (N1235 and N1354). Surprisingly, plasma ADAMTS13 derived peptides containing the N-linked sites N142, N146, N707 and N1354 were also detected in the non-PNGase F treated ADAMTS13 samples, suggesting that N-glycosylation at these residues is not complete. Interestingly, for recombinant ADAMTS13 all N-glycosylation peptides were detected only in the PNGase F treated samples. These findings suggest that N-glycosylation of plasma ADAMTS13 is more heterogenous when compared to recombinant ADAMTS13. The tryptic peptide containing the predicted N-linked glycosylation site at N828 was not identified in both plasma and recombinant ADAMTS13. Therefore we were unable to determine whether a glycan is attached to this residue. Mammalian N-linked moieties are highly versatile in nature. Lectin binding analysis of both plasma and recombinant ADAMTS13 revealed that both proteins contain high mannose structures, sialic acid and galactose residues (Figure S5). Absence of binding of peanut agglutinin (PNA), a lectin that binds the disaccharide galactose-β(1–

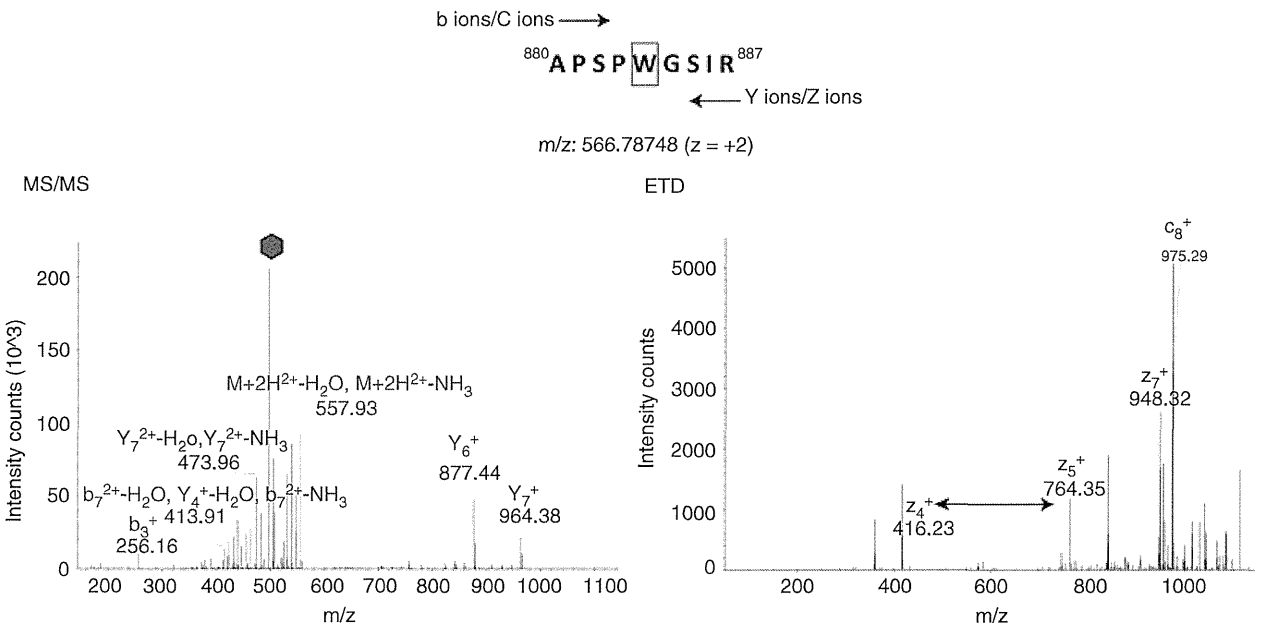

Fig. 6. Putative C-mannosylation of TSR domains of ADAMTS13. CID and ETD fragmentation spectrum of ADAMTS13 derived peptides. Left panel show the MS/MS spectrum of the APSPWGSIR peptide belonging to the TSR4 domain of ADAMTS13. The major peak in the spectrum corresponds to the neutral loss (120 Da) of a cross-ring fragmentation product potentially derived from a C-mannosylated Trp (indicated by the red hexagon). The peak corresponding to the intact peptide is indicated in green; selected peaks corresponding to b- and y-ions are indicated in red and blue. Right panel shows the ETD spectrum of the APSPWGSIR peptide. Differences between z5+ and z4+ ions allowed for identification of the modified Trp at position 884.

3)-N-acetylgalactosamine, to plasma derived ADAMTS13 might be due to the modification of the core structure by the addition of sugars such as sialic acid and/or fucose (Figure S5). Removal of sialic acid and/or fucose might therefore be necessary in order to allow binding of the PNA lectin to plasma derived ADAMTS13. Overall our findings suggest that plasma ADAMTS13 contains different terminal glycan structures when compared to recombinant ADAMTS13 (Figure S5) and suggests the presence of complex glycan structures on plasma ADAMTS13.

O-fucosylation is a different post translational modification in which fucose or the disaccharide glucose-β1,3-fucose is covalently attached to Ser or Thr residues within a putative consensus sequence CSX(S/T)CG [4,20]. It is well established that O-fucosylation takes place in TSRs [4,16,20]. Previous studies have identified several putative O-fucosylation moieties in the TSR domains of recombinant ADAMTS13 [4,21]. Through a combination of CID/ETD MS/MS analysis we provide evidence for neutral loss of Hex, dHex and Hex-dHex sugar moieties suggesting the presence of six putative O-fucosylation sites within the TSR2, TSR3, TSR5, TSR6, TSR7 and TSR8 domains of plasma ADAMTS13. As expected no putative O-fucosylation site was identified in the TSR1 since that region does not contain a consensus sequence. We were unable to identify the peptide containing the putative O-fucosylation site from the TSR4 domain of ADAMTS13 and therefore cannot exclude the possibility of such modification in this domain. MS/MS fragmentation spectra (Fig. 3; Figure S6 and S7) showed a characteristic neutral loss of a hexose-deoxyhexose disaccharide (308 Da) confirming the presence of the glycan within the TSR derived peptides. To further identify the site of glycosylation we performed an ETD analysis. Unlike CID analysis, ETD fragmentation does not remove the glycan from the peptide allowing for assignment of the modified residue [22–24]. Using this approach we were able to assign the exact site of modification for three of the TSRs glycosylated peptides: S698 for GPCSVSCGAGLR, S907 for TGAQAAHVWTPAAG SCSVSCGR and S1087 for WHVGTWMECSVSCGD-GIQR (Fig. 5; Figure S8). Unfortunately the precise site of glycosylation for the remaining peptides could not be identified due to low sequence coverage. Taking into account previous findings of putative O-fucosylated sites in recombinant ADAMTS13 [4] and the consensus sequence of the modification we suggest that O-fucosylation takes place at S757, S965 and S1027.

In addition to N- and O-linked oligosaccharides, proteins are often modified by C-mannosylation. C-mannosylation is a common post-translation modification of TSR [16,18]. In this study we show that Trp884 and Trp390 in the TSR 4 and TSR 1 domain of both plasma and recombinant are potentially modified by C-mannosylation, suggesting that this modification might not only occur within the consensus sequence (WXXW) but also takes place at other sites [18]. Recently, Akiyama and co-workers showed that Trp387 in TSR1 was C-mannosylated in a recombinant ADAMTS13 variant [25]. Our data suggest that

Trp390 in plasma derived ADAMTS13 contains a putative C-mannosylation site. Interestingly, ions corresponding to putative C-mannosylated WSSWGPR peptide were identified that did not contain the mannose-residue at Trp390. This suggest that Trp387 might also be modified in plasma derived ADAMTS13. However, the fragmentation spectrum did not allow for accurate assignment of the putative C-mannosylation at Trp387 (data not shown). In a recent study, Ling and co-workers showed that replacement of Trp387 by Ala resulted in a reduced expression and processing activity of ADAMTS13 suggesting that C-mannosylation might be required for optimal folding [26].

Protein glycosylation has not only been considered to play an important role in cell-cell communication and adhesion, protein structural stability, membrane structure and cellular signaling. Several studies have shown that protein glycans may be crucial also for T-cell recognition of autoantigens in autoimmune disorders [10]. Previously we have shown that antigen presenting cells derived from HLA-DRB1*11-positive individuals present a CUB2 domain derived peptide FINVAPHARIA (residues 1327–1338) [27]. Since HLA-DRB1*11 is considered to be a risk factor for the development of acquired TTP [28–30] functional presentation of this CUB2 domain-derived peptide might contribute to the onset of acquired TTP [27]. Presentation of the FINVAPHARIA peptide (residues 1327–1338) may potentially be affected by the presence of an N-linked glycan at N1354. Moreover, non-DRB1*11 donors present a second CUB domain peptide ASYILIRDTHSLRTTA (residues 1355–1370) which is right adjacent to N1354 [27]. This raises the possibility that differential glycosylation at N1354 might contribute to the onset of acquired TTP in patients capable of presenting such peptides.

Addendum

N. Sorvillo performed experiments, analyzed data, made the figures and wrote the paper. P. Kaijen, C. van der Zwaan, F. Verbij, W. Pos, M. Matsumoto performed experiments. Y. Fujimura and M. Matusmoto provided protocols and prepared large amounts of antibody for purification of ADAMTS13 from plasma. A. B. Meijer and J. Voorberg designed research, analyzed the data, wrote and reviewed the paper. R. Fijnheer designed research and reviewed the paper.

Acknowledgements

Dr. Hendrik Feys is kindly acknowledged for providing anti-TSR5-8 monoclonal antibody 20D2.

Funding

This study was supported by grant PPOC-08-021. Grant support from Takeda Medical Foundation is gratefully acknowledged.

Disclosure of Conflict of Interest

The authors state that they have no conflict of interests.

Supporting Information

Additional Supporting Information may be found in the online version of this article:

Fig. S1. Purification of pADAMTS13.
Fig. S2. Sequence coverage of ADAMTS13.
Fig. S3. Mapping of N-linked glycosylation sites in plasma ADAMTS13.
Fig. S4. Mapping of N-linked glycosylation sites in recombinant ADAMTS13.
Fig. S5. Identification of terminal N-linked glycans in both plasma and recombinant ADAMTS13.
Fig. S6. Identification of putative O-fucosylation sites in TSR domains of plasma derived ADAMTS13.
Fig. S7. Identification of putative O-fucosylation sites in TSR domains of recombinant ADAMTS13.
Fig. S8. Identification of putative O-fucosylation sites in TSR domains of plasma derived ADAMTS13.
Fig. S9. Putative C-mannosylation of TSR1 domain of plasma ADAMTS13.
Fig. S10. Putative C-mannosylation of TSR1 and TSR4 domains of recombinant ADAMTS13.

References

1 Moake JL. Thrombotic thrombocytopenic purpura: the systemic clumping "plague". *Annu Rev Med* 2002; **53**: 75–88.
2 Zheng X, Chung D, Takayama TK, Majerus EM, Sadler JE, Fujikawa K. Structure of von Willebrand factor-cleaving protease (ADAMTS13), a metalloprotease involved in thrombotic thrombocytopenic purpura. *J Biol Chem* 2001; **276**: 41059–63.
3 Dong JF. Cleavage of ultra-large von Willebrand factor by ADAMTS-13 under flow conditions. *J Thromb Haemost* 2005; **3**: 1710–6.
4 Ricketts LM, Dlugosz M, Luther KB, Haltiwanger RS, Majerus EM. O-fucosylation is required for ADAMTS13 secretion. *J Biol Chem* 2007; **282**: 17014–23.
5 Zhou W, Tsai HM. N-Glycans of ADAMTS13 modulate its secretion and von Willebrand factor cleaving activity. *Blood* 2009; **113**: 929–35.
6 Pos W, Luken BM, Sorvillo N, Kremer Hovinga JA, Voorberg J. Humoral immune response to ADAMTS13 in acquired thrombotic thrombocytopenic purpura. *J Thromb Haemost JTH* 2011; **9**: 1285–91.
7 Motto DG, Chauhan AK, Zhu G, Homeister J, Lamb CB, Desch KC, Zhang W, Tsai HM, Wagner DD, Ginsburg D. Shigatoxin triggers thrombotic thrombocytopenic purpura in genetically susceptible ADAMTS13-deficient mice. *J Clin Invest* 2005; **115**: 2752–61.
8 Kremer Hovingas JA, Lämmle B. Role of ADAMTS13 in the pathogenesis, diagnosis, and treatment of thrombotic thrombocytopenic purpura. *Hematology Am Soc Hematol Educ Program* 2012; **2012**: 610–6.
9 Purcell AW, van Driel IR, Gleeson PA. Impact of glycans on T-cell tolerance to glycosylated self-antigens. *Immunol Cell Biol* 2008; **86**: 574–9.

10 Szabo TG, Palotai R, Antal P, Tokatly I, Tothfalusi L, Lund O, Nagy G, Falus A, Buzas EI. Critical role of glycosylation in determining the length and structure of T cell epitopes. *Immunome Res* 2009; **5**: 4.
11 Hanisch F-G, Schwientek T, von Bergwelt-Baildon MS, Schultze JL, Finn O. O-Linked glycans control glycoprotein processing by antigen-presenting cells: a biochemical approach to the molecular aspects of MUC1 processing by dendritic cells. *Eur J Immunol* 2003; **33**: 3242–54.
12 Ishioka GY, Lamont AG, Thomson D, Bulbow N, Gaeta FC, Sette A, Grey HM. MHC interaction and T cell recognition of carbohydrates and glycopeptides. *J Immunol* 1992; **148**: 2446–51.
13 Pos W, Crawley JT, Fijnheer R, Voorberg J, Lane DA, Luken BM. An autoantibody epitope comprising residues R660, Y661, and Y665 in the ADAMTS13 spacer domain identifies a binding site for the A2 domain of VWF. *Blood* 2010; **115**: 1640–9.
14 Hiura H, Matsui T, Matsumoto M, Hori Y, Isonishi A, Kato S, Iwamoto T, Mori T, Fujimura Y. Proteolytic fragmentation and sugar chains of plasma ADAMTS13 purified by a conformation-dependent monoclonal antibody. *J Biochem (Tokyo)* 2010; **148**: 403–11.
15 Hofsteenge J, Huwiler KG, Macek B, Hess D, Lawler J, Mosher DF, Peter-Katalinic J. C-Mannosylation and O-Fucosylation of the Thrombospondin Type 1 Module. *J Biol Chem* 2001; **276**: 6485–98.
16 Gonzalez de Peredo A, Klein D, Macek B, Hess D, Peter-Katalinic J, Hofsteenge J. C-mannosylation and o-fucosylation of thrombospondin type 1 repeats. *Mol Cell Proteomics* 2002; **1**: 11–8.
17 Wang LW, Dlugosz M, Somerville RP, Raed M, Haltiwanger RS, Apte SS. O-fucosylation of thrombospondin type 1 repeats in ADAMTS-like-1/punctin-1 regulates secretion: implications for the ADAMTS superfamily. *J Biol Chem* 2007; **282**: 17024–31.
18 Wang LW, Leonhard-Melief C, Haltiwanger RS, Apte SS. Post-translational modification of thrombospondin type-1 repeats in ADAMTS-like 1/punctin-1 by C-mannosylation of tryptophan. *J Biol Chem* 2009; **284**: 30004–15.
19 Zubarev RA, Kelleher NL, McLafferty FW. Electron capture dissociation of multiply charged protein cations. A nonergodic process. *J Am Chem Soc* 1998; **120**: 3265–6.
20 Luo Y, Nita-Lazar A, Haltiwanger RS. Two distinct pathways for O-fucosylation of epidermal growth factor-like or thrombospondin type 1 repeats. *J Biol Chem* 2006; **281**: 9385–92.
21 Akiyama M, Takeda S, Kokame K, Takagi J, Miyata T. Crystal structures of the noncatalytic domains of ADAMTS13 reveal multiple discontinuous exosites for von Willebrand factor. *Proc Natl Acad Sci U S A* 2009; **106**: 19274–9.
22 Chalkley RJ, Thalhammer A, Schoepfer R, Burlingame AL. Identification of protein O-GlcNAcylation sites using electron transfer dissociation mass spectrometry on native peptides. *Proc Natl Acad Sci U S A* 2009; **106**: 8894–9.
23 Perdivara I, Deterding LJ, Cozma C, Tomer KB, Przybylski M. Glycosylation profiles of epitope-specific anti-β-amyloid antibodies revealed by liquid chromatography-mass spectrometry. *Glycobiology* 2009; **19**: 958–70.
24 Lin Z, Lo A, Simeone DM, Ruffin MT, Lubman DM. An N-glycosylation Analysis of Human Alpha-2-Macroglobulin Using an Integrated Approach. *J Proteomics Bioinform* 2012; **5**: 127–34.
25 Akiyama M, Nakayama D, Takeda S, Kokame K, Takagi J, Miyata T. Crystal structure and enzymatic activity of an ADAMTS13 mutant with the East Asian-specific P475S polymorphism. *J Thromb Haemost* 2013; **11**: 1399–406.
26 Ling J, Su J, Ma Z, Ruan C. The WXXW motif in the TSR1 of ADAMTS13 is important for its secretion and proteolytic activity. *Thromb Res* 2013; **131**: 529–34.
27 Sorvillo N, van Haren SD, Kaijen PH, Ten Brinke A, Fijnheer R, Meijer AB, Voorberg J. Preferential HLA-DRB1*11 dependent presentation of CUB2 derived peptides by ADAMTS13 pulsed dendritic cells. *Blood* 2013; **121**: 3502–10.
28 Scully M, Brown J, Patel R, McDonald V, Brown CJ, Machin S. Human leukocyte antigen association in idiopathic thrombotic thrombocytopenic purpura: evidence for an immunogenetic link. *J Thromb Haemost* 2010; **8**: 257–62.
29 Coppo P, Busson M, Veyradier A, Wynckel A, Poullin P, Azoulay E, Galicier L, Loiseau P. HLA-DRB1*11: a strong risk factor for acquired severe ADAMTS13 deficiency-related idiopathic thrombotic thrombocytopenic purpura in Caucasians. *J Thromb Haemost* 2010; **8**: 856–9.
30 John ML, Hitzler W, Scharrer I. The role of human leukocyte antigens as predisposing and/or protective factors in patients with idiopathic thrombotic thrombocytopenic purpura. *Ann Hematol* 2012; **91**: 507–10.

Pediatr Nephrol (2015) 30:603–608
DOI 10.1007/s00467-014-2975-4

ORIGINAL ARTICLE

Eculizumab in the treatment of atypical hemolytic uremic syndrome in an infant leads to cessation of peritoneal dialysis and improvement of severe hypertension

Toshiyuki Ohta · Kohtaro Urayama · Yoshihiro Tada · Takeki Furue · Sayaka Imai · Keita Matsubara · Hiroaki Ono · Takashi Sakano · Kazuhiko Jinno · Yoko Yoshida · Toshiyuki Miyata · Yoshihiro Fujimura

Received: 1 August 2014 / Revised: 10 September 2014 / Accepted: 11 September 2014 / Published online: 16 October 2014

Abstract
Background Severe hypertension (HTN) and acute kidney injury frequently associated with atypical hemolytic uremic syndrome (aHUS) were refractory to various therapies in the pre-eculizumab era. Here we report the case of a 4-month-old boy who developed aHUS presenting with undetectable C3 protein, no predisposing mutations in complement factors, and no antibodies against factor H.
Methods Repeated plasma infusions and nine sessions of plasmapheresis were ineffective. The patient initially required continuous hemodiafiltration and thereafter peritoneal dialysis. Despite vigorous antihypertensive treatment and improved fluid overload with dialysis, HTN persisted. His low C3 level (<20 mg/dl) suggested unrestricted complement activation. Therefore, based on the suspicion of unrestricted complement cascade in the pathogenesis, treatment with eculizumab, a human anti-C5 monoclonal antibody, was initiated with the aim of controlling disease activity.
Results Eculizumab therapy resulted in the control of severe HTN and cessation of peritoneal dialysis.
Conclusions This infant with HTN and acute kidney injury associated with aHUS was treated successfully with eculizumab.

Keywords Plasmapheresis-resistant · Meningococcal infection · Prophylactic antibiotics · Vaccination · Pathological findings · Atypical hemolytic uremic syndrome · Anti-C5 therapy

T. Ohta (✉) · T. Furue
Department of Pediatric Nephrology, Hiroshima Prefectural Hospital, 1-5-54 Ujina-Kanda, Minami-ku, Hiroshima city, Hiroshima 734-8530, Japan
e-mail: t-ohta@hph.pref.hiroshima.jp

K. Urayama · S. Imai · K. Matsubara · H. Ono · T. Sakano · K. Jinno
Department of Pediatrics, Hiroshima Prefectural Hospital, Minami-ku, Hiroshima city, Hiroshima, Japan

Y. Tada
Department of Critical Care, Hiroshima Prefectural Hospital, Minami-ku, Hiroshima city, Hiroshima, Japan

Y. Yoshida · Y. Fujimura
Department of Blood Transfusion Medicine, Nara Medical University, Kashihara, Nara, Japan

T. Miyata
Department of Molecular Pathogenesis, National Cerebral and Cardiovascular Center, Suita, Osaka, Japan

Introduction

Hemolytic uremic syndrome (HUS) is a rare disease with manifestations of microangiopathic hemolytic anemia, thrombocytopenia, and renal impairment. There are two types of HUS: HUS which follows a diarrheal infection often caused by Shiga toxin-producing *Escherichia coli* (Stx-HUS) and atypical HUS (or non-Stx-HUS) caused by one or more genetic mutations. The latter type is extremely rare—accounting for less than 10 % of all HUS cases—and the clinical outcome is unfavorable, with up to one-half of cases progressing to end-stage renal failure and one-fourth of patients dying in the acute phase if they do not receive rigorous treatment [1]. Historically, the first-line therapy for aHUS has been plasma therapy, including plasmapheresis [2, 3]. However, approximately 80 % of patients with aHUS have only partial responses to short-term plasmapheresis with subsequent persistent tissue damage [4]. The main pathogenesis of aHUS is unrestricted overactivation of the alternative pathway of complement activation [5], which has led to eculizumab, a human anti-C5 monoclonal antibody, being used for both

plasmapheresis-resistant and plasmapheresis-dependent cases of aHUS [6–9].

We here report a 4-month-old male baby with plasmapheresis-resistant aHUS who was successfully treated with eculizumab. The results of this very effective therapy was control the patient's extremely severe hypertension and cessation of peritoneal dialysis.

Case report

A severely ill 4-month-old male baby weighing 7.1 kg presented with a 2-day history of fever and vomiting. His father and mother were alive and in good health; his maternal grandmother and grandaunt had died of cerebral infarction, but no details were available. Laboratory tests at a local hospital revealed anemia (8.9 g/dl), thrombocytopenia (64 × 10^9/l), and acute renal insufficiency consistent with HUS. He was transferred to Hiroshima University Hospital where upon admission, schistocytes on the peripheral blood film, elevated levels of lactate dehydrogenase (LDH; 1,830 U/l), creatinine (1.95 mg/dl), and urea (38.8 mg/dl), and decreased platelets level (41 × 10^9/l) were detected. Stool culture was negative, and immunoglobulin M (IgM) antibody for O-157 lipopolysaccharide was not detected. A tentative diagnosis of aHUS was made, which was later confirmed by a normal test result for ADAMTS13 (72 %) activity. After admission to the hospital, the patient received multiple blood transfusions, including fresh frozen plasma and continuous hemodiafiltration. However, his general condition remained poor, and hemolytic anemia, elevated LDH, and renal failure did not improve.

On day 26 he was transferred to the Hiroshima Prefectural Hospital for closer management of the renal failure. On admission, the serum complement of C3 and C4 was <20 and 14 (normal range 13–35) mg/dl, respectively. On the third day of admission, plasmapheresis with 60 ml/kg of fresh frozen plasma was initiated and performed for 3 consecutive days, in combination with hemodiafiltration, followed by plasmapheresis every other day for the next 2 weeks; however, there was no remarkable improvement of the hemolysis and renal failure. After nine sessions of plasmapheresis, the patient was not in remission from his disease according to the guideline of the European Pediatric Study Group for HUS [2]. Moreover, his severe hypertension (systolic blood pressure 140–150 mmHg), which initially did not respond to fluid removal by hemodiafiltration, was also refractory to the treatment with an intravenous large dose of nicardipine chloride, peroral enarapril, and losartan. At that time, eculizumab was not licensed for the treatment of aHUS in Japan. Therefore, after receiving approval from the institutional ethics committee, we started the patient on eculizumab, with an initial dose of 300 mg administered on day 48, followed by a second dose of 300 mg on day 55; thereafter and up to the present (17 months), the patient has been receiving one 300-mg dose of eculizumab every 3 weeks in accordance with the manufacturer's recommendations, with sustained remission. For the prevention of infection after the treatment with eculizumab, the patient has received continuous antibiotic prophylaxis with cefdinir from the first administration of eculizumab, and on days 62 and 169 he received tetravalent conjugate meningococcal vaccine (Menactra®; Sanofi Pasteur, Lyon, France).

The severe hypertension gradually improved, and the patient was switched from intravenous nicardipine chloride to peroral nifedipine 11 weeks after the first administration of eculizumab. Plasma renin activity on days 40, 60, 84, and 123 was 18, 77, 5.7, and 1.2 ng/ml/h, respectively. Renal function improved, and peritoneal dialysis (PD) was stopped on day 117. On day 108 the patient presented with white stool and jaundice. Liver function tests were consistent with cholestatic jaundice with a total bilirubin of 2.5 mg/dl, direct bilirubin of 1.7 mg/dl, aspartate transaminase (AST) of 1,337 U/l, alanine transaminase (ALT) of 1,667 U/l, LDH of 954 U/l, and gamma-glutamyl transferase (GTP) of 1,093 U/l. Abdominal ultrasonography revealed dilatation of the common bile duct and some gallstones. Magnetic resonance cholangiopancreatograpy confirmed the diagnosis of cholelithiasis, which regressed spontaneously (Fig. 1).

Genetic work-up showed no predisposing mutations in complement factor (CF) H, CFI, CFB, C3, thrombomodulin, or membrane cofactor protein. At the initiation of the first session of plasmapheresis, protein level and CFH activity were normal, and antibodies to CFH were undetectable. Membrane cofactor protein expression on peripheral blood mononuclear cells was within the normal limit. Cobalamin-C disorder was ruled out based on the normal level of homocystine in the urine and negative tandem mass screening test.

A kidney ultrasound on admission to our hospital showed normal-sized kidneys for age with increased echogenicity in the renal cortex. A kidney biopsy performed on day 159 showed mild swelling of the glomerular endothelium and decrease in the size of the lumen, with approximately 10% of interstitial cell infiltration and fibrosis. A small number of fragmented erythrocytes were observed in a few glomeruli among the 47 glomeruli assessed (Fig. 2b). Only rarely were wrinkling, collapse, and/or thickening of the glomerular basement membranes, identical to that observed in ischemic lesions, observed in the biopsy specimen. However, a few glomeruli showed partial duplication of the peripheral basement membrane, which is a marker of chronic change. Moreover, several intralobular arteries and arterioles had a narrowed lumen due to myointimal hyperplasia (Fig. 2a). Juxtaglomerular apparatus hyperplasia was also observed in some glomeruli (Fig. 2a). Immunofluorescence findings showed weak C3, fibrinogen, and IgM depositions in glomerular capillaries.

Currently, 17 months after the initiation of eculizumab administration, the laboratory test results of our patient are